The International Journal of Advanced Manufacturing Technology
https://doi.org/10.1007/s00170-017-1570-9

ORIGINAL ARTICLE

Influence of the time step selection on dynamic simulation of milling operation

Edouard Rivière-Lorphèvre[1] · **Hoai Nam Huynh**[2] · **Olivier Verlinden**[2]

Received: 9 March 2017 / Accepted: 28 December 2017

Abstract
Simulation of manufacturing processes also called virtual manufacturing plays a key role for the optimisation of productivity. Among all the manufacturing processes, machining operations are often unavoidable because most of the mechanical parts need to be machined during their production cycle, at least for finishing operations. The development of machining simulation is still challenging due to large strains, strain rates and temperatures needing complex material flow stress laws for example. In order to model industrially relevant situations, macroscopic approaches are often used to keep a reasonable simulation time. The simulation of milling operations at a macroscopic level combines a mechanistic model of the cutting forces, a numerical model of the dynamic response of the machine tool and a geometric model predicting the shape of the machined part. A numerical integration procedure is used to obtain the time history of the forces and the vibrations occurring during machining. This paper presents two different approaches for the consideration of the cutting force into the integration procedure and discusses the time step selection used to perform this numerical integration. By taking the evolution of the cutting force into account through a single integration step, it is possible to increase the time step. For a given precision, it is possible to reduce the computation time by a factor up to ten using this approach.

Keywords Machining simulation · Numerical integration · Chatter vibrations

1 Introduction

The simulation of machining processes is an unavoidable technique for optimisation of productivity. The reduction of setup time allowed by these techniques is essential to maintain competitiveness of industrial manufacturers. In addition, some high added value sectors need the production of parts difficult to machine due to their complex shapes, their low rigidity or the use of materials with low machinability. Great benefits can be obtained from numerical expertise.

The first model of machining operation has been proposed by Tlusty [1] in the sixties. It was based on linearisation of the turning process in order to model the regenerative effect leading to chatter vibration. The stability lobe diagram, locating the combination of depth of cut and spindle speed producing stable operation, is the main outcome of this approach. It was later extended to milling operations by several authors [2–4].

Stability analysis of the delay differential equation governing the machining simulation has been another proficient research topic. This approach improves the simulation for small immersion operations where a second type of instability linked to flip bifurcation can be observed [5–9]. These simulation methods are able to model simple geometrical configurations with a relatively low computing time. In addition, these methods are often well suited to compute the stability lobes in an efficient way.

With the rise of computing power, the simulation of the machining operation with a full numerical model has been

✉ Edouard Rivière-Lorphèvre
edouard.riviere@umons.ac.be

Hoai Nam Huynh
hoainam.huynh@umons.ac.be

Olivier Verlinden
olivier.verlinden@umons.ac.be

[1] Machine Design and Production Engineering, University of Mons, Place du parc 20, 7000 Mons, Belgium

[2] Theoretical Mechanics, Dynamics and Vibrations, University of Mons, Place du Parc 20, 7000 Mons, Belgium

Published online: 11 January 2018

more and more accessible [10]. Models based on finite element method [11], Arbitrary Lagrangian/Eulerian method [12], meshless methods [13] among others have been studied. However, the complete simulation of machining operations by numerical models based on finite element is nowadays so complex that only academic examples such as 2D plane strain approach can be simulated with a reasonable computing time [14].

In order to model industrial applications, a good compromise is to use a macroscopic approach to model the interaction between the cutting tool and the workpiece [15, 16]. The actual geometry of the tool and the precise toolpath can be studied with reasonable simulation time taking several non-linearities into account. Stability analysis [16–18], prediction of cutting forces with complex tool geometry [19, 20] or development of stabilisation techniques [21, 22] can be achieved by this approach although they require higher CPU time than the methods based on the analysis of the delay differential equations previously presented. A dynamic model is implemented as part of the simulations presented in this paper.

Extension of macroscopic models have been recently developed to be able to deal with complex geometry of the part (pocket milling [23], thin walled structure [24, 25] e.g.). Further developments were carried out to use more precise model of cutting forces [26, 27] and to take the uncertainty of the process into account [28]. Parasite effects such as the deflection of the cutting tool [29] can be reduced. This allows the generalisation of the simulation to micro milling operations [30]. Finally, a complete virtual model of machine tool can be developed prior to its physical prototyping [31] opening the way to full virtual prototyping of the machining operations.

The information about the exact integration procedure is sometimes difficult to obtain from the literature. Some authors do not specify the integration method nor the use of iteration on a single time step (see [18] or [32] for example). Several authors use different integration schemes to simulate milling operation such as fourth order Runge-Kutta [33, 34], Euler's method [35] or Newmark's method [17]. In most papers, few comments are made on the choice of the integration time step. Ming et al. [32] proposed a criterion based on the highest frequency of the simulated structure, Peigne et al. [17] added a geometrical criterion ensuring that there are enough time steps to model precisely the interaction between the tool and the workpiece for any given tool revolution.

This paper aims to study two different integration approaches for the simulation of milling operations in order to determine guidelines for the selection of the integration time step. Two examples using several cutting conditions are presented leading to simulations of stable and unstable machining operations.

2 Description of the numerical model

Dynamic simulation of milling operation is based on the coupling of three main models: the model of the surface, computing the amount of material removed by the cutting tool and predicting the surface finish; the model of the cutting forces, modelling the interaction between the tool and the workpiece; and the dynamic model of the system, predicting the vibrations occurring in the tool and the workpiece due to the cutting forces. Those models are combined in a single environment to simulate the machining process.

2.1 Surface modelling

Chatter vibration is a regenerative process produced by the fact that the cutting edges remove material from a previously machined surface [1]. Hence, the surface model must be accurate enough to take this effect into account. The approach used in this paper is based on a $2\frac{1}{2}\ D$ model considering that the cutting tool moves only within a plane perpendicular to its axis. An 'eraser of matter' model proposed by Peigne et al. [17] is used during the simulation. The surface is approximated by its profile in different positions along the axis of the cutter by a list of points (Fig. 1).

An intersection procedure is set up to compute the undeformed chip thickness (Fig. 2). The movement of the cutting edge between two time steps is approximated by a second order Bézier spline linking the position of the cutting edge at the current time step and its two previous positions. This procedure needs to be repeated on every segment defining the surface till an actual intersection is found. It is a time-consuming part in the whole process. It might be interesting to use it as sparsely as possible.

During the simulation of machining, the area of material swept during a given time step must be removed from the workpiece. The amount of data needed to save the geometry of the surface at each time step is so high that only its current state is saved during the simulation. It means that when a

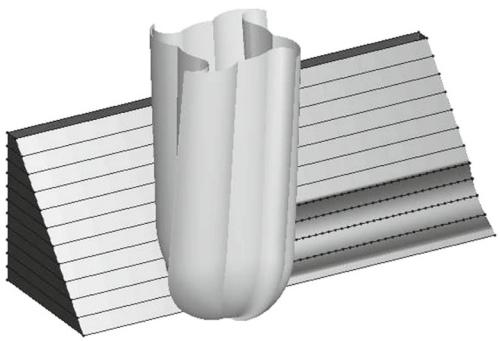

Fig. 1 Machined surface and its decomposition in profiles

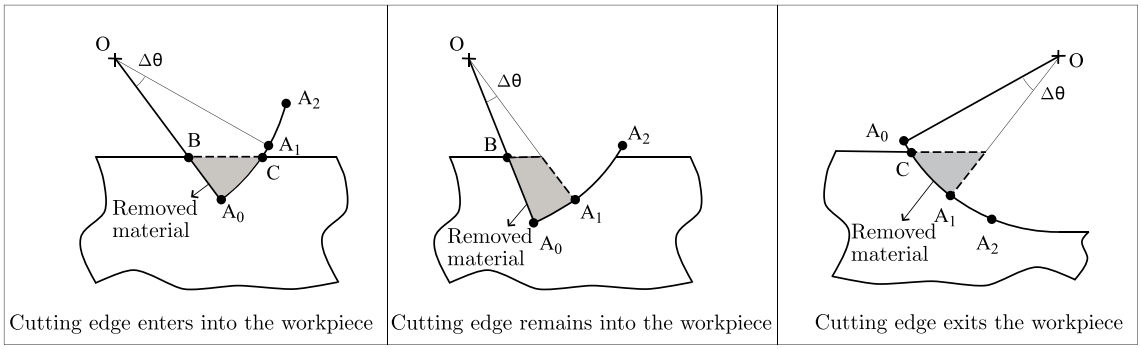

Fig. 2 Algorithm used to model the machined surface (inspired from [17])

computation step is performed, it is impossible to come back to a previous state. However, during any given time step, the integration procedure can be iterated in order to converge before continuing the integration procedure.

2.2 Cutting force modelling

Macroscopic modelling of cutting forces in machining issues from so-called mechanistic models. These models allow the prediction of the cutting forces for a given tool/material couple using simple analytical laws. Complex cutter shapes are divided into several slices along their revolution axis in order to approximate the geometric data [19]. The most common model proposed by Kienzle [36] computes the cutting forces on a local frame (t along the cutting speed, r along the local normal to the tool and a along the third direction leading to an orthogonal frame with t and r) as functions of the undeformed chip thickness h and the height of a slice da as

$$dF_i = K_i \cdot h^n \cdot da \tag{1}$$

with $i = \{r, t, a\}$ and n an exponent smaller than or equal to one.

Altintas and Lee [37] proposed another popular model by adding the effect of friction along the local length of the cutting edge dS as

$$dF_i = K_{i,c} \cdot h \cdot da + K_{i,e} \cdot dS \tag{2}$$

The local contributions are projected on a common reference frame using the rotation angle of the cutting edge ϕ and the orientation of the local normal to the cutter κ (Fig. 3):

$$\begin{Bmatrix} dF_x \\ dF_y \\ dF_z \end{Bmatrix} = \begin{bmatrix} -\cos\phi & -\sin\phi \cdot \sin\kappa & -\sin\phi \cdot \cos\kappa \\ \sin\phi & -\cos\phi \cdot \sin\kappa & -\cos\phi \cdot \cos\kappa \\ 0 & -\cos\kappa & -\sin\kappa \end{bmatrix} \cdot \begin{Bmatrix} dF_t \\ dF_r \\ dF_a \end{Bmatrix} \tag{3}$$

All these contributions are then summed up along the cutting edges to obtain the resultant cutting force (F_x, F_y and F_z) in the reference frame.

2.3 Dynamic behaviour of the machine

The dynamic behaviour of the machine tool can be modelled by several techniques such as the modal identification of the frequency response function at the tooltip by modal analysis, physical modelling of the machine tool as a multibody system or a finite element model of the machine tool.

Modal model is fully experimental and can be used when few information is available on the machine itself. It can be used for determination of optimal cutting parameters [38] but not for virtual CNC approach. Modal technique can be completed using receptance coupling [39] to avoid multiple experimental fitting for several tools.

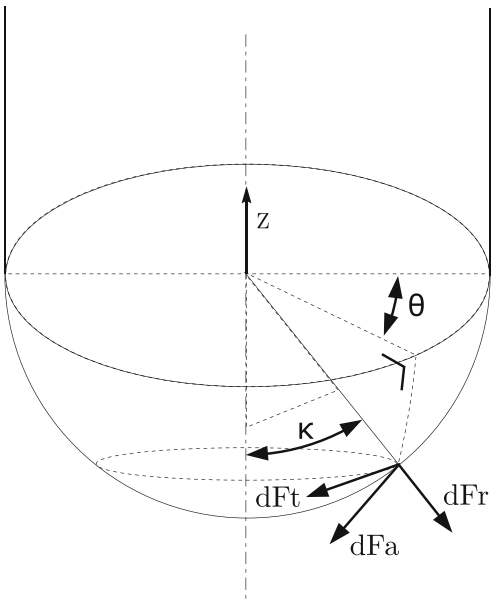

Fig. 3 Local frame for the cutting forces

In order to enrich the possibilities of simulation, multibody approach [40, 41] can be used to model the machine tool. The response of the machine can be taken into account with finer details (effect of the control loop on stability for example); however, it needs a better understanding of the machine manufacturing and can be more complicated to set up.

2.4 Numerical integration

The motion of a mechanical system can be described by the governing equation:

$$\mathbf{M}\left(\underline{\mathbf{q}}\right)\cdot\underline{\ddot{\mathbf{q}}}+\underline{\mathbf{h}}\left(\underline{\mathbf{q}},\underline{\dot{\mathbf{q}}}\right)=\underline{\mathbf{g}}\left(\underline{\mathbf{q}},\underline{\dot{\mathbf{q}}},t\right) \tag{4}$$

where $\underline{\mathbf{q}}$ is the vector gathering the configuration parameters of the system, $\underline{\dot{\mathbf{q}}}$ and $\underline{\ddot{\mathbf{q}}}$ its first and second time derivatives, $\mathbf{M}$ the mass matrix, $\underline{\mathbf{h}}$ the contribution of centrifugal, gyroscopic and Coriolis effects and $\underline{g}$ the external forces.

These equations can be rewritten as:

$$\mathbf{M}\left(\mathbf{q}\right)\cdot\underline{\ddot{\mathbf{q}}}+\underline{\mathbf{H}}\left(\underline{\mathbf{q}},\underline{\dot{\mathbf{q}}},t\right)=f\left(\underline{\mathbf{q}},\underline{\dot{\mathbf{q}}},\underline{\ddot{\mathbf{q}}},t\right)=0 \tag{5}$$

with $\underline{\mathbf{H}}\left(\underline{\mathbf{q}},\underline{\dot{\mathbf{q}}},t\right)=\underline{\mathbf{h}}\left(\underline{\mathbf{q}},\underline{\dot{\mathbf{q}}}\right)-\underline{\mathbf{g}}\left(\underline{\mathbf{q}},\underline{\dot{\mathbf{q}}},t\right)$. The numerical integration considers that the time is discretised in time steps and configuration parameters and their time derivatives are evaluated at each time step. The computation of position and velocity from the acceleration is made from Newmark's integration formulas:

$$q^{t+h}=q^{t}+h\dot{q}^{t}+\left(0.5-\beta\right)h^{2}\ddot{q}^{t}+\beta h^{2}\ddot{q}^{t+h} \tag{6}$$

$$\dot{q}^{t+h}=\dot{q}^{t}+\left(1-\gamma\right)h\ddot{q}^{t}+\gamma h\ddot{q}^{t+h} \tag{7}$$

where β and γ are parameters and h the time step. In order to ensure unconditional stability for linear systems, γ and β parameters must be selected in the following range:

$$\gamma\geq 0,5 \tag{8}$$

$$\beta\geq 0,25\cdot\left(\gamma+0,5\right)^{2} \tag{9}$$

For this paper, value $\gamma=0.5$ and $\beta=0.25$ have been selected, ensuring that no numerical damping is added in the process. The equations of motion are built in their residual form from the kinematics and the applied forces. The integration consists in computing the equations of motion (5) in terms of the accelerations at time $t+h$ after having replaced the positions q (6) and the velocities $\dot{q}$ (7) by their Newmark's integration formulas:

$$f\left(\underline{\Lambda}\left(\underline{\mathbf{q}}^{t},\underline{\dot{\mathbf{q}}}^{t},\underline{\ddot{\mathbf{q}}}^{t},\underline{\ddot{\mathbf{q}}}^{t+h}\right),\ \underline{\tilde{\Lambda}}\left(\underline{\mathbf{q}}^{t},\underline{\dot{\mathbf{q}}}^{t},\underline{\ddot{\mathbf{q}}}^{t},\underline{\ddot{\mathbf{q}}}^{t+h}\right),\underline{\ddot{\mathbf{q}}}^{t+h},t+h\right)=0 \tag{10}$$

where $\underline{\Lambda}$ and $\underline{\tilde{\Lambda}}$ are the expression of position and speed at the next time step as a function of the acceleration. With this substitution, the only remaining unknowns are the accelerations $\underline{\ddot{q}}$:

$$\underline{\mathbf{F}}\left(\underline{\ddot{\mathbf{q}}}^{t+h}\right)=0 \tag{11}$$

The solution of this equation is found using Newton-Raphson method to achieve the convergence of the acceleration $\ddot{\mathbf{q}}$ for each configuration parameter at time $t+h$ as

$$\underline{\ddot{\mathbf{q}}}^{t+h,n}=\underline{\ddot{\mathbf{q}}}^{t+h,n-1}-\mathbf{J}^{-1}\cdot\underline{\mathbf{F}}\left(\underline{\ddot{\mathbf{q}}}^{t+h,n-1}\right) \tag{12}$$

with $\underline{\mathbf{F}}\left(\underline{\ddot{\mathbf{q}}}^{t+h}\right)$ the equation of motion and $\mathbf{J}$ the Jacobian matrix of Eq. 11 with respect to the unknown accelerations. Convergence is obtained when

$$\left\|\underline{\ddot{\mathbf{q}}}^{t+h,n}-\underline{\ddot{\mathbf{q}}}^{t+h,n-1}\right\|\leq\epsilon \tag{13}$$

with ϵ the tolerance. If the external force is a constant and the dynamic system is linear, Eq. 11 can be solved in a closed form.

3 Numerical integration procedure

While performing simulation of milling operations, time step is generally selected based on two constraints:

- It should be small enough to accurately simulate the high frequency response, usually a choice of one tenth of the smallest period of the system is chosen [32].
- It should be small enough for being able to model the machined surface accurately, a classical choice is to use at least 30 time steps between the entry end the exit of the tool within the workpiece [17].

When a machine tool is used, the second constraint is often dominant, thus a rather small time step is used from the dynamic point of view. It means that the difference of position of the cutting edge between two successive time steps is small. It is then usually admitted that the cutting force remains constant over the time step, in order to speed up the simulation by avoiding multiple computations of the intersection between the cutter and the workpiece. If larger time steps are used, the variation of the cutting force over the time step has to be taken into account.

3.1 Single pass algorithm

The first proposed algorithm considers a single computation of the intersection with the workpiece at each time step. The cutting force is computed from the undeformed chip thickness evaluated with the kinematic of the system only. The additional displacement provided by the dynamic response of the system is neglected. It is called the 'single pass algorithm' afterwards. The cutting force is only

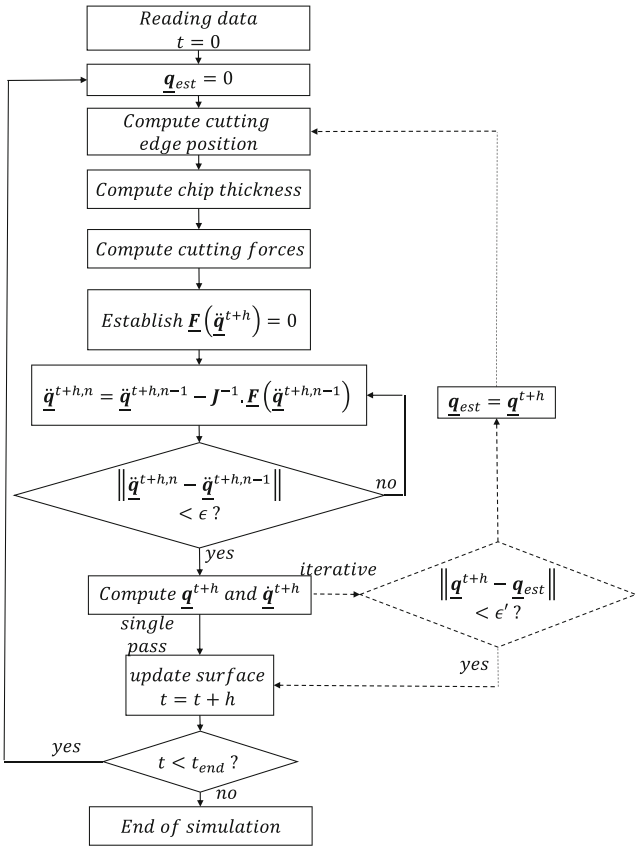

Fig. 4 Numerical integration algorithm

computed at the beginning of the time step. Figure 4 shows (in plain lines) the principle of this method.

The assumption that cutting forces are kept constant during each time step may be a limitation for some cases, for example:

- If the structure is highly flexible so that high amplitude vibration can be observed.
- If the system has an unstable behaviour.

The second point may be considered as marginal as far as the objective of the simulation is to determine cutting conditions that lead to a stable behaviour. However, the accurate simulation of unstable machining operations is an important field of study in order to develop precise detection of vibration [42–44] and methods able to stabilise the system [21, 45, 46].

3.2 Iterative algorithm

During the numerical integration of the equations of motion, the first predicted position of the cutting edge is only determined by considering the kinematics of the machine. A corrected position can be found by taking the dynamics of the system into account (Fig. 5). This leads to a

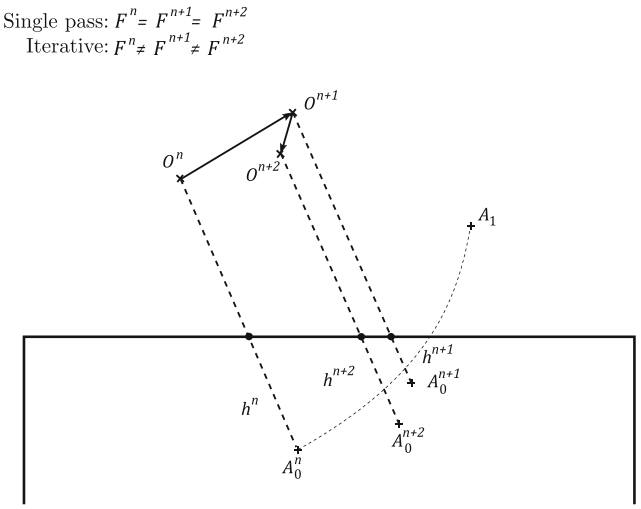

Fig. 5 Successive iterated positions of the tool center during the convergence loop

slightly different position of the cutting edges, modifying accordingly the value of the cutting force. The cutting force evaluated at the beginning of the time step can be updated, leading to a new estimation of the position of the cutting edge. The computation of a single time step thus needs to iterate the intersection procedure until the position of the cutting edge has converge within a given tolerance (a value of 0.1 μm is used in this paper). Once the convergence is achieved, the surface is updated before the computation of the next time step. This procedure taking the variation of the cutting force during a single time step with respect to the cutter position is called the 'iterative algorithm' afterwards.

This iterative algorithm thus includes multiple calls to the intersection procedure in the loop as shown in Fig. 4 (dashed lines).

4 Application of the method

In order to test the influence of the integration procedure and the impact of the time step selection, two numerical examples were selected [3, 47]. The simulated results have been validated by different references in the literature [48, 49]. Several simulations were performed to assess the general behaviour of the system over different cutting conditions and the influence of the time step selection over the results of the simulation.

4.1 Milling simulation with a SDOF system

The first simulated testcase is taken from [50]:

- Cutting tool: cylindrical endmill with one tooth;

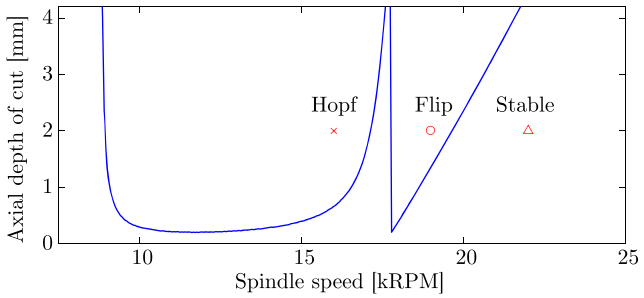

Fig. 6 Stability lobes diagram for the testcase

- Workpiece: 7075-T6 aluminium alloy (K_t = 550 MPa, K_r = 200 MPa)
- Dynamic response of the system: 1 mode along feed direction with an eigenfrequency of 146.5 Hz, a damping ratio of 0.32% and a modal mass of 2.573 kg;
- Cutting conditions: half immersion upmilling, feed of 0.05 mm/tooth, spindle speed ranging from 5000 to 25,000 rpm, axial depth of cut from 0.1 to 4.5 mm.

The stability of the system is described by the so-called stability lobe diagram (SLD) that shows the division between stable and unstable milling operations on a spindle speed/ axial depth of cut (ADOC) chart. Two types of instabilities can be observed: one linked to the Hopf bifurcation which is observed for roughing and finishing operations and one linked to the flip bifurcation which is mainly observed for finishing operations.

Figure 6 shows the SLD for the selected testcase. For an axial depth of cut of 2 mm, three particular spindle speeds have been selected leading to three different behaviours:

- A stable case at a spindle speed of 22,000 rpm;
- Two unstable cases:
  - one linked to Hopf bifurcation at a spindle speed of 16,000 rpm;
  - one linked to flip bifurcation at a spindle speed of 19,000 rpm.

Figure 7 shows typical evolution of the cutting forces and vibrations amplitude for these cases. The results are similar to those observed in the literature [51].

The aim of this section is to describe the evolution of the results in order to deduce the general trends for the selection of the time step. For each case, a reference simulation has been performed with a time step ensuring the convergence of the results.

4.1.1 Chatter-free

For a spindle speed of 22,000 rpm with an axial depth of cut of 2 mm, the milling system is stable. The dominant criterion to select the default time step for integration is the geometric one. The use of 120 steps per revolution leads to a value $h_0 = 2.27 \cdot 10^{-5}\ s$ (or a sample frequency of 34 kHz). Using this time step value, it can be observed that there is no significant difference on the results obtained by both integration methods (Fig. 8). The simulation of 300 revolutions of the cutter is completed in less than 1 s using a laptop with a I3-2310M CPU (2.10 GHz) and 4 Gb of RAM.

The vibration has a small amplitude with a dominant frequency linked to the tooth passing frequency of 366.67 Hz as expected [47]. The choice of a smaller time step does not change the results of the simulation meaning that the default time step is sufficient for the convergence of the results.

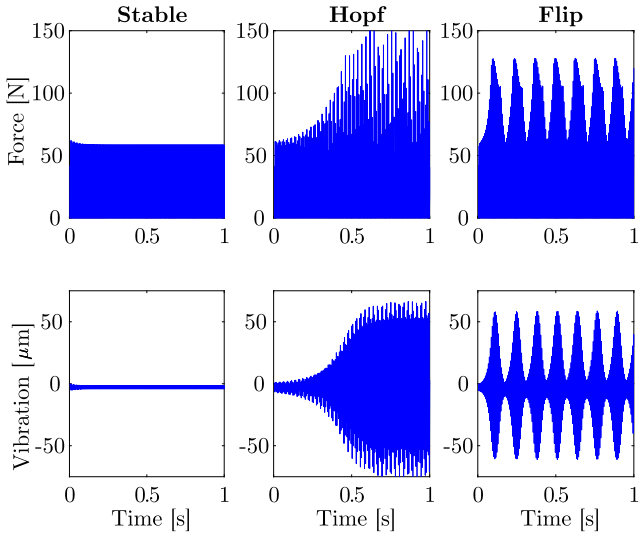

Fig. 7 Typical evolution of cutting forces and vibrations for stable (left), Hopf unstable (center) and flip unstable (right) simulations

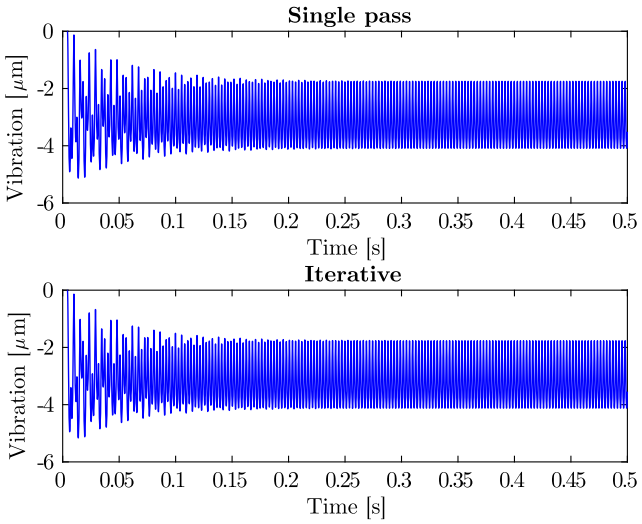

Fig. 8 Vibration amplitude for a stable testcase (top: single pass algorithm, bottom: iterative algorithm)

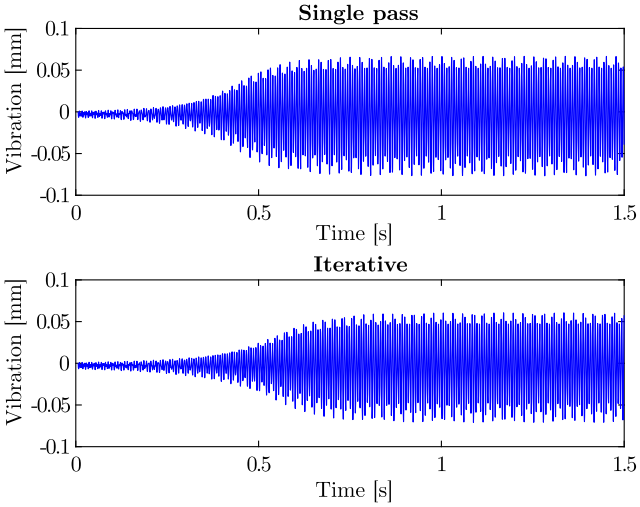

Fig. 9 Vibration amplitude for an unstable testcase with Hopf bifurcation (top: single pass algorithm, bottom: iterative algorithm)

4.1.2 Hopf bifurcation

At a spindle speed of 16,000 rpm and 2 mm ADOC, the system has an unstable behaviour linked to Hopf bifurcation. Several simulations were performed during 300 revolutions of the cutter with both integration procedures starting with the reference time step h_0. Once more, the most severe criterion is the geometric one for this case with a value of $3.12 \cdot 10^{-5}$ s (sample frequency of 32 kHz). For this case, the results of the simulations using both methods show some differences (Fig. 9). It can be noticed that the time delay to reach an unstable state slightly differs from one simulation to another.

Two indicators were selected to assess the quality of the results: the dominant frequency of the displacement signal which is the main chatter frequency and the peak to peak (ptp) amplitude of the displacement signal as proposed by Smith [2]. The converged values for these indicators are 0.12365 mm for ptp amplitude and 153.1 Hz for the chatter frequency. Tables 1 and 2 show the evolution of these indicators linked to the CPU time for a selection of time steps. The same laptop was used to perform the simulations. Less time steps were tested with the iterative procedure because the convergence of the results was already achieved with a time step divided by 30 whereas the single pass procedure needed a reduction of 300.

Table 1 Summary of the results for Hopf bifurcation (single pass algorithm)

h_0/h	ptp (mm)	f_{chatter} (Hz)	CPU time (s)
0.5	0.1525	151.6	1
1	0.1395	152.3	3
3	0.1299	153.1	13
10	0.1256	153.1	77
30	0.1243	153.1	207
100	0.1239	153.1	1211
300	0.1237	153.1	10,516

Table 2 Summary of the results for Hopf bifurcation (iterative algorithm)

h_0/h	ptp (mm)	f_{chatter} (Hz)	CPU time (s)
0.5	0.1182	153.1	1,5
1	0.1216	153.1	4
3	0.1231	153.1	24
10	0.1235	153.1	140
30	0.1236	153.1	420

The results show that each simulation accurately predicts the chatter frequency. The peak to peak evolution with respect to the time step is shown in Fig. 10. The single pass algorithm tends to overestimate this indicator while the iterative method tends to underestimate it. Convergence of the peak to peak amplitude is observed for both integration methods. The evolution of CPU time with respect to the time step is nearly quadratic. For a given choice of time step, the single pass procedure has a smaller CPU time as expected. It can be noticed that for the same choice of time step the ratio of CPU time is around two between both procedures.

Figure 11 shows the evolution of the gap between the simulated peak to peak amplitude and the converged value with respect to the simulation time. It can be observed that the iterative procedure gives results that are closer to the reference for a given simulation time. For a given precision,

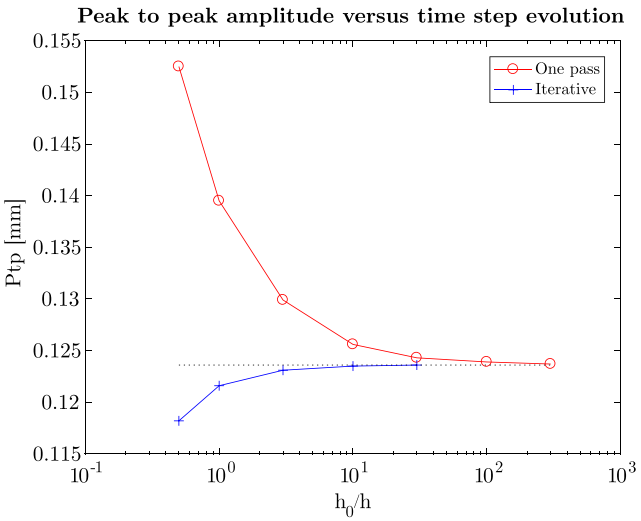

Fig. 10 Evolution of the peak to peak amplitude with respect to the time step (dotted line represent the converged value)

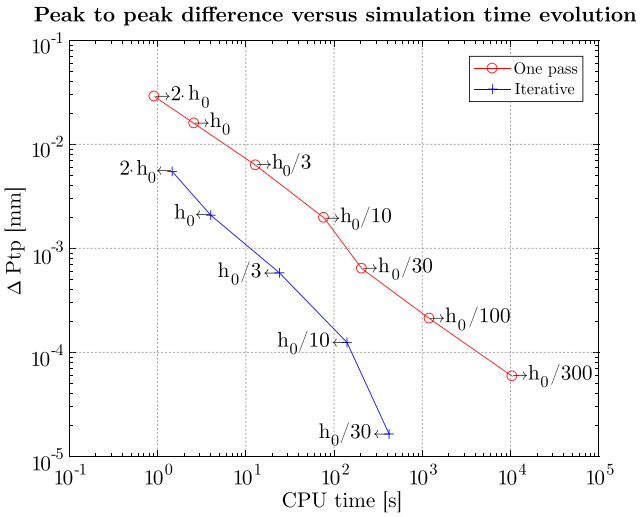

Fig. 11 Gap between simulated peak to peak amplitude and reference value

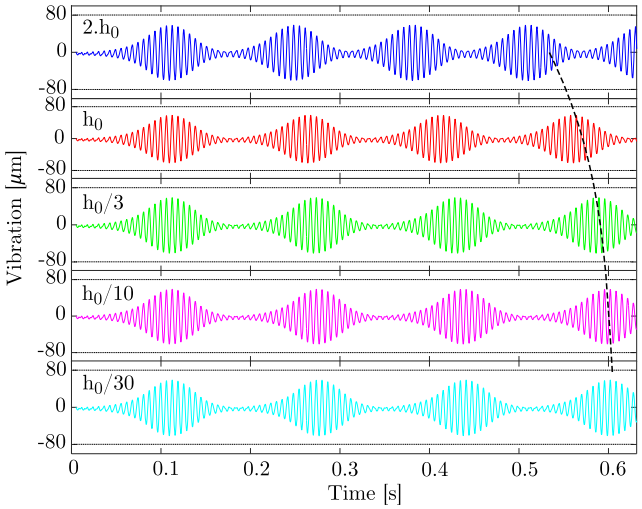

Fig. 13 Evolution of simulated vibration for the unstable flip case with time steps ranging from $2 \cdot h_0$ to $h_0/30$

the iterative procedure can use a time step ten times larger than the single pass procedure leading to similar results. Using the reference time step, the single pass algorithm computes a peak to peak amplitude that differs from the converged value of more than 10%. With the same time step, the results of the iterative differs of less than 2%. It shows that the reference time step is a good compromise while using the iterative algorithm.

4.1.3 Flip bifurcation

The same procedure was applied on the flip unstable case. The spindle speed is now 19,000 rpm with 2 mm ADOC and 300 revolutions of the cutter are simulated. The reference time step h_0 is now $2.63 \cdot 10^{-5}$ s (sample frequency 38 kHz), still computed using the geometric criterion. Reaching an instability linked to the flip bifurcation causes the displacement of the tool to double its period leading to a modulated movement [47]. Two interesting frequencies can be tracked: the chatter frequency and a lower modulated frequency (Fig. 12), the same laptop was used to perform the simulations.

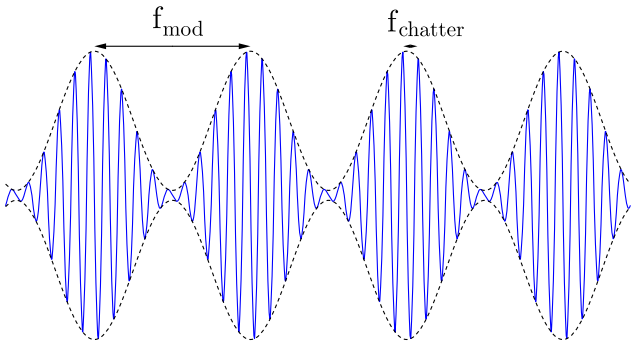

Fig. 12 Typical displacement of the tool during flip bifurcation instability

Figure 13 shows the evolution of the simulated signal for single pass integration scheme with different time steps. It can be observed that the modulated frequency content of the signal tends to differ significantly.

The modulated frequency criterion was added to those previously used in order to select the suitable time step while comparing the two integration procedures. The converged values are 0.350 mm for the ptp amplitude, 155.24 Hz for the chatter frequency and 6.21 Hz for the modulated frequency. Tables 3 and 4 summarise the results.

It can be noticed that for flip bifurcation, the chatter frequency (Fig. 14) and the peak to peak amplitude are close to the reference values with the reference time step.

The modulated frequency (Fig. 15) has a higher relative variation and it is necessary to use a time step three to ten times smaller than the reference value to reach an error smaller than 5%.

The single pass algorithm tends to overestimate this value while the iterative algorithm underestimates it (Fig. 16). This is usually observed for implicit numerical integration

Table 3 Results for flip bifurcation using single pass algorithm

h_0/h	ptp (mm)	$f_{chatter}$ (Hz)	f_{mod} (Hz)	CPU time (s)
1	0.351	154.41	7.72	0.6
3	0.350	154.92	6.73	3
10	0.350	155.14	6.46	15
30	0.350	155.21	6.21	44
100	0.350	155.21	6.21	246
300	0.350	155.24	6.21	2164

Table 4 Results for flip bifurcation using iterative algorithm

h_0/h	ptp (mm)	f_{chatter} (Hz)	f_{mod} (Hz)	CPU time (s)
0.5	0.355	158.32	5.03	0.4
1	0.351	155.86	5.65	1
3	0.350	155.39	5.97	5
10	0.350	155.29	5.97	30
30	0.350	155.24	6.21	90

that tends to lower the frequencies while explicit methods tend to rise the frequencies.

4.2 Milling simulation with a MDOF system

In order to test the integration method on a more complex dynamic system, another milling example taken from [3] is used:

- Cutting tool: cylindrical shell mill of 4 in. diameter with eight teeth;
- Workpiece: aluminium alloy (K_t = 1500 MPa, K_r = 450 MPa)
- Dynamic response of the system: two modes in both feed (x) and perpendicular (y) directions, the identified modal data of the system are summarised in Table 5. ;
- Cutting conditions: half immersion upmilling, feed of 0.1 mm/tooth, spindle speed from 1000 to 8000 rpm, axial depth of cut from 1 to 11 mm.

The FRF of the dynamic system in both directions is shown in Fig. 17. There is one dominant mode in each direction. The stability lobes are given in Fig. 18. The stability is mainly conditioned by the second mode in x direction.

The selected cutting parameters are 2000 rpm spindle speed and 5 mm ADOC. These cutting parameters lead to an unstable operation linked to Hopf bifurcation. The reference time step h_0 is now $2.5 \cdot 10^{-4}$ s (sample frequency of 4 kHz), still computed using the geometric criteria. Tables 6 and 7 present the results of simulation along 50 revolutions of the tool. The reference value for ptp amplitude is 0.118 mm along x direction and 0.151 mm along y direction. The dominant frequency at 397.08 Hz turns out to be the same in both x and y directions. This frequency is linked to the second mode along the feed direction.

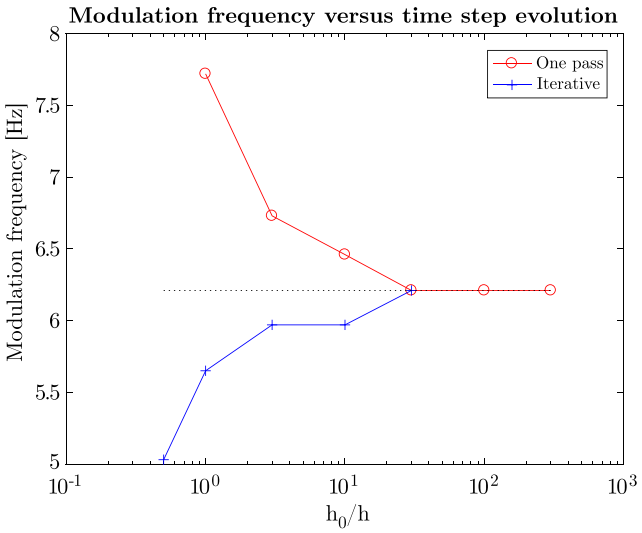

Fig. 15 Modulated frequency with respect to time step (dotted line is the converged value)

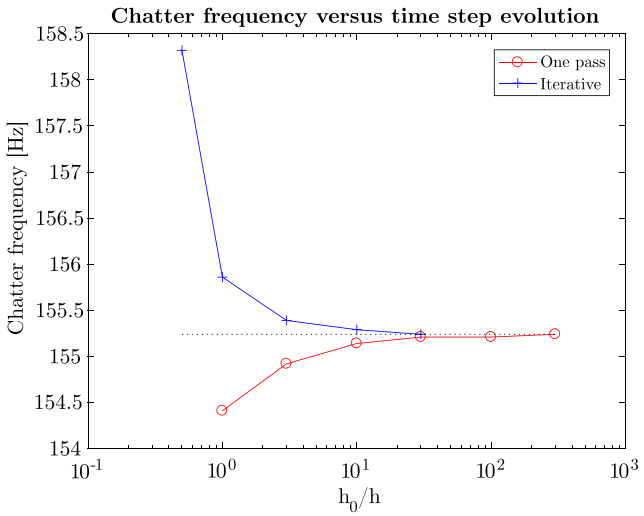

Fig. 14 Chatter frequency with repect to time step (dotted line is the converged value)

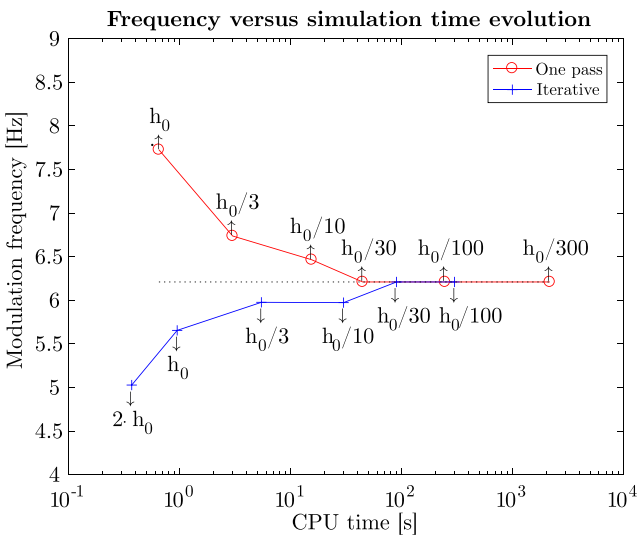

Fig. 16 Evolution of modulated frequency with respect to CPU time

Table 5 Dynamic properties of the MDOF milling system

	Mode	f (Hz)	ξ	k (N/m)
x	1	260	0.12	2.26E+08
	2	389	0.04	5.54E+07
y	1	150	0.1	2.13E+08
	2	348	0.1	2.14E+07

Figure 19 shows that with the default time step, the single pass algorithm produces results completely different from the converged value. For $\frac{h_0}{h} = 0.5$ and $\frac{h_0}{h} = 1$, the displacement along x direction has a dominant frequency of 266.66 Hz corresponding to the tooth passing frequency for the eight teeth (2000 rpm $\cdot 8/60$).

The analysis of the FFT for both cases (Fig. 20) confirms that the frequency content is different for both approaches. With the single pass algorithm, the dominant frequency peaks are linked to the tooth passing frequency and its harmonics, which is a typical feature of a stable system [49]. With the iterative algorithm, the main frequency is close to one eigenfrequency of the system.

It seems that while using an inappropriate time step with the single pass procedure, the level of vibrations is underestimated, so a system with an unstable behaviour remains stable from a numerical point of view. This confirms the interest of the iterative procedure for a more reliable simulation.

While using a time step smaller than the default one, all simulations produce a dominant frequency with the right order of magnitude.

The peak to peak amplitude in both directions (Fig. 21) converges while the time step decreases. For this case, both methods tend to underestimate the converged value. The gap between simulated and reference peak to peak amplitude

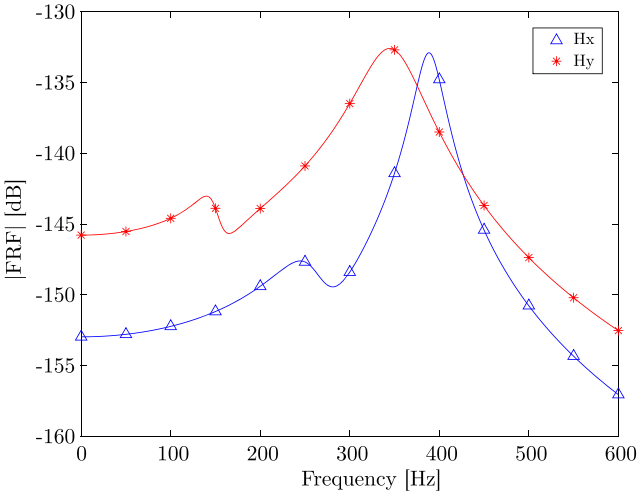

Fig. 17 FRF in both directions for MDOF system

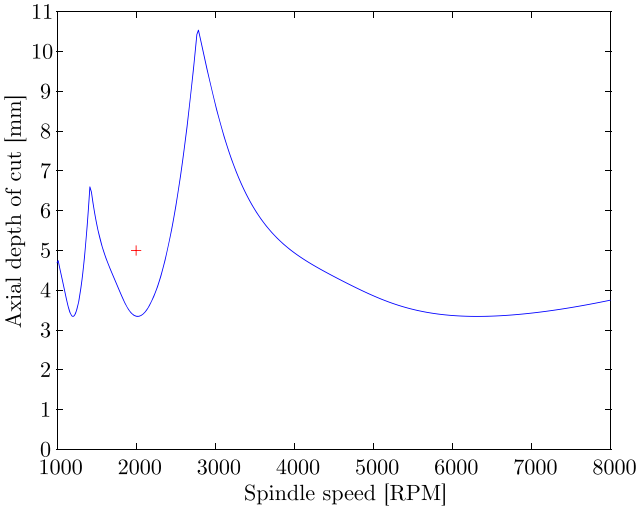

Fig. 18 Stability lobes for the MDOF milling example

along x (Fig. 22) and y direction (Fig. 23) follows the same trend as for the SDOF example. Once again, for a given precision, the iterative procedure allows the reduction of the CPU time by a factor of ten.

4.3 Milling simulation with a non symmetrical dynamic system

4.3.1 High spindle speed example

The dynamic behaviour of a milling machine is often dominated by the behaviour of the spindle. This may explain the fact that most of the time, the FRF of the system is nearly symmetrical for both x and y directions. However, it can be useful to test the results of simulations for a non-symmetrical system. For this purpose, a third testcase taken from [52] has been selected:

- Cutting tool: cylindrical endmill of 3.175 mm diameter with two teeth.
- Workpiece: aluminium alloy (Kt = 1378 MPa, Kr = 861 MPa)

Table 6 Simulation of 2 DOF system with one pass algorithm

h_0/h	ptp_x (mm)	ptp_y (mm)	f_{chatter} (Hz)	CPU time (s)
0.5	0.025	0.085	266.67	0.5
1	0.034	0.081	266.67	1
3	0.067	0.109	387.56	2
10	0.094	0.129	394.15	9
30	0.108	0.142	395.62	54
100	0.113	0.148	396.35	133
300	0.115	0.149	397.08	365

Table 7 Simulation of 2 DOF system with iterative algorithm

h/h_0	ptp_x (mm)	ptp_y (mm)	f_{chatter} (Hz)	CPU time (s)
0.5	0.073	0.116	266.67	1.5
1	0.093	0.128	386.82	2
3	0.106	0.138	395.61	6
10	0.115	0.149	397.08	26
30	0.116	0.151	397.08	106

– Dynamic response of the system: three modes in both feed (x) and perpendicular (y) directions, the identified modal data of the system are summarised in Table 8, showing a shift of more than 200 Hz between the modes in both directions.
– Cutting conditions: slot milling, feed of 0.1 mm/tooth, spindle speed 30,000 rpm, axial depth of cut 60 μm.

The default time step is $3.333 \cdot 10^{-5}$ s (sample frequency of 30 kHz.

The combination of axial depth of cut and spindle speed leads to a unstable behaviour linked to Hopf bifurcation. Tables 9 and 10 show the results of simulations along 200 revolutions of the cutter. The results are graphically presented in Figs. 24 and 25. For this testcase, both integration procedures tend to underestimate the chatter frequency.

Even though this example has a dynamic system with a non-symmetrical behaviour and has higher frequencies modes, the main conclusions are the same as previously stated:

– For a given time step selected, the iterative method gives more precise results.

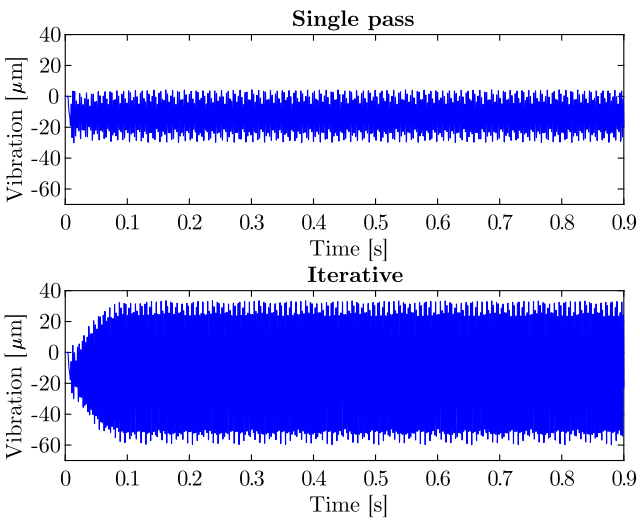

Fig. 19 Evolution of the displacement along feed direction using the default time step

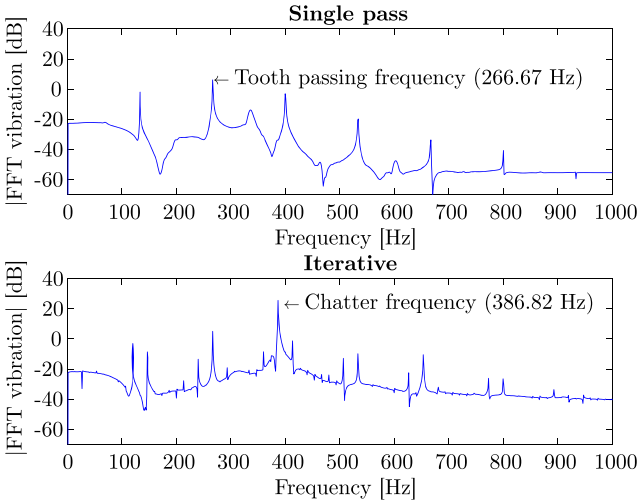

Fig. 20 FFT of the displacement along feed direction using the default time step

– For a given CPU time, the iterative method gives more precise results than the one pass algorithm;
– the use of the default time step with the iterative procedure give a good compromise between reasonable CPU time and good precision.

4.4 Stability lobes

In order to evaluate the impact on a broader range of cutting parameters, the SLD was simulated using the dynamic simulation method and the data of the SDOF example with the default time step. The studied domain was discretised in a series of points and a dynamic simulation was performed for each point. An instability criterion has to be used to

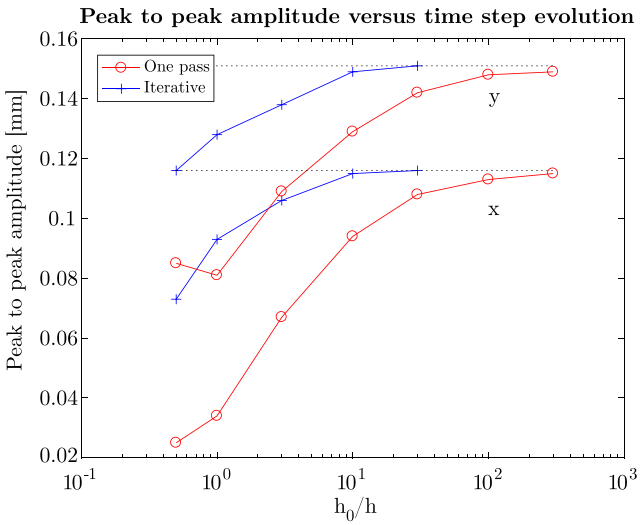

Fig. 21 Simulated peak to peak amplitude evolution with respect to the time step

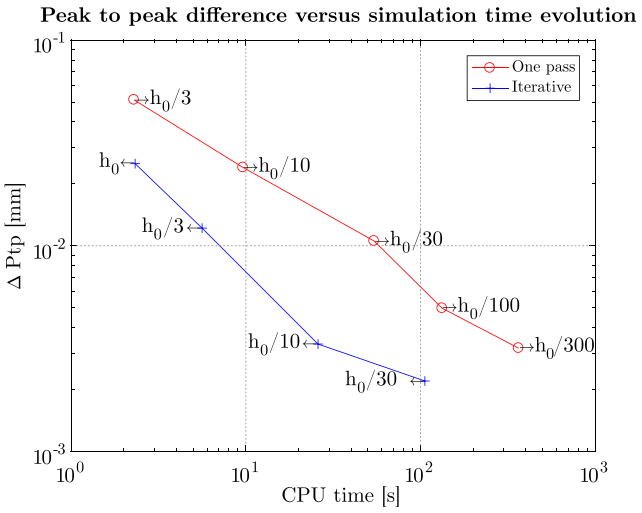

Fig. 22 Gap between simulated peak to peak amplitude and reference value along x direction

separate stable and unstable simulations. Classically, the comparison is made on the maximal undeformed chip thickness computed during the simulations. If this value exceeds 125% of the value observed for a stable simulation, the system is considered unstable [18].

The SLD is plotted using the value of axial depth of cut that separate stable and unstable simulations. Figure 26 shows the comparison of the stability lobes obtained using both integration procedures with the default value of the time step (120 steps per revolution).

There is no modification of the lobes linked to the flip bifurcation and a slight effect on the lobe linked to the Hopf bifurcation. This difference is mainly linked to the

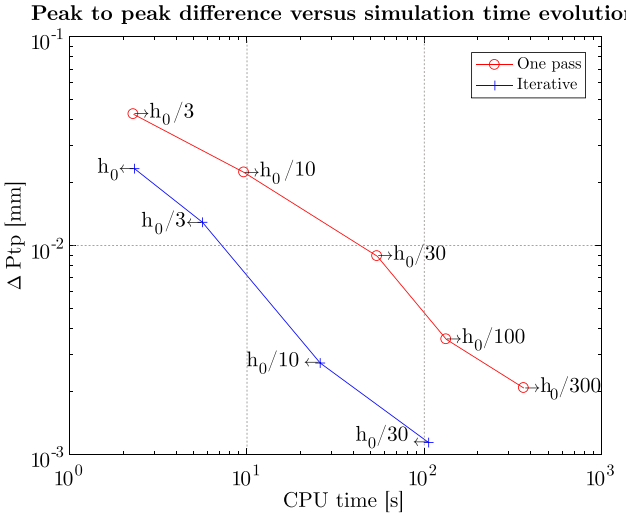

Fig. 23 Gap between simulated peak to peak amplitude and reference value along y direction

Table 8 Dynamic properties of the MDOF milling system

	Mode	f (Hz)	ξ	k (N/m)
	1	241	0.054	4.91E+6
x	2	383	0.058	1.46E+7
	3	2277	0.155	1.62E+5
	1	56.6	0.142	1.64E+7
y	2	142	0.055	3.62E+7
	3	2558	0.097	2.36E+5

previously mentioned difference on the delay to establish unstable behaviour of the system. As far as the simulation time is limited to a finite number of tool revolutions, it might be possible that for borderline simulation points, the instability criterion is not reached at the end of the simulation for an unstable example. This may be linked to the fact that iterative methods tend to add a bit of numerical damping that might delay the appearance of instability. In order to illustrate this effect, Fig. 27 shows the evolution of the cutting forces and the vibrations for a point at 17,000 rpm spindle speed and 2.4 mm ADOC. The dashed line shows the end of the simulation while considering 500 revolutions of the cutter. It can be seen that this leads to a fault detection of a stable simulation for the iterative procedure.

Figures 28, 29 and 30 show the evolution of the peak to peak amplitude with respect to the axial depth of cut for the three spindle speeds that were previously selected. These results confirm the previously observed trends:

- for unstable cutting conditions linked to Hopf bifurcation, there is a significant difference in ptp amplitude according to the integration procedure;
- for unstable cutting conditions linked to flip bifurcation, there is no significant difference on the ptp indicator;
- for stable cutting conditions, there is no significant difference between both integration methods.

Table 9 Simulation of 3 DOF system with one pass algorithm

h_0/h	ptp_x (μm)	ptp_y (μm)	f_{chatter} (Hz)	CPU time (s)
0.5	0.48413	0.12562	2150	0.4
1	0.52413	0.14671	2276	1.27
3	0.221012	0.096468	2361.8	7.81
10	0.16472	0.079221	2376.8	84
30	0.15248	0.072857	2381.9	430
100	0.15303	0.071908	2386.9	1587
300	0.15079	0.72264	2387	124,285

Table 10 Simulation of three DOF system with iterative algorithm

h_0/h	ptp_x (μm)	ptp_y (μm)	f_{chatter} (Hz)	CPU time (s)
0.5	0.095968	0.053383	2320.8	0.92
1	0.11872	0.065302	2371.5	2.35
3	0.14504	0.070976	2387	14.79
10	0.14623	0.071229	2386.9	153
30	0.15075	0.072281	2387	791

5 Summary

In this paper, a simulation framework for milling operation has been presented, linking a multimode dynamic system with a mechanistic model of machining. Two different integration algorithms are tested neglecting or considering the variation of the cutting force during a step of computation. The iterative integration approach, taking this variation into account, allows the use of a larger time step while maintaining the accuracy of the results.

The quality of the results has been analysed for different time steps over various cutting conditions. The main conclusions are as follows:

- For stable simulation case, there is no significant effect of the integration procedure on the result.
- For unstable simulation case linked to Hopf bifurcation, the chatter frequency is accurately predicted by both procedure. The reduction of the time step allows a better prediction of the peak to peak amplitude of the unstable vibration. For a given CPU time, the iterative procedure is more precise than the single-pass one.
- For unstable simulation case linked to flip bifurcation, the chatter frequency and the peak to peak amplitude of vibration are accurately predicted by both procedures. The modulated frequency linked to period doubling is less precisely predicted and a reduction of the time step is necessary to reach convergence of the results.

Generally speaking, although having a small effect on the simulation time, the iterative integration procedure allows using bigger time steps for similar accuracy of the results. It allows the reduction of CPU time by a factor up to ten for a given simulation of milling operation.

Several guidelines can thus be proposed for the selection of the time step in dynamic simulation of milling operations:

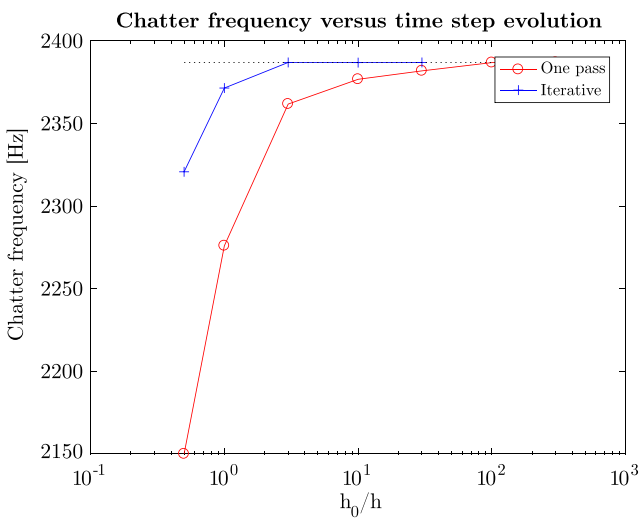

Fig. 24 Simulated chatter frequency evolution with respect to the time step

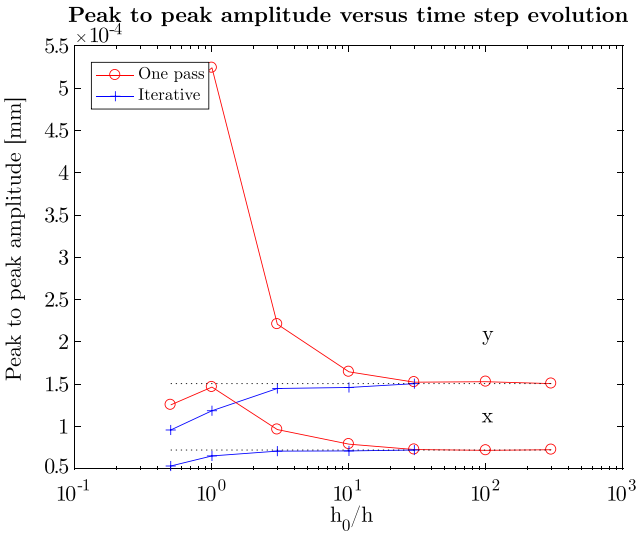

Fig. 25 Simulated peak to peak amplitude evolution with respect to the time step

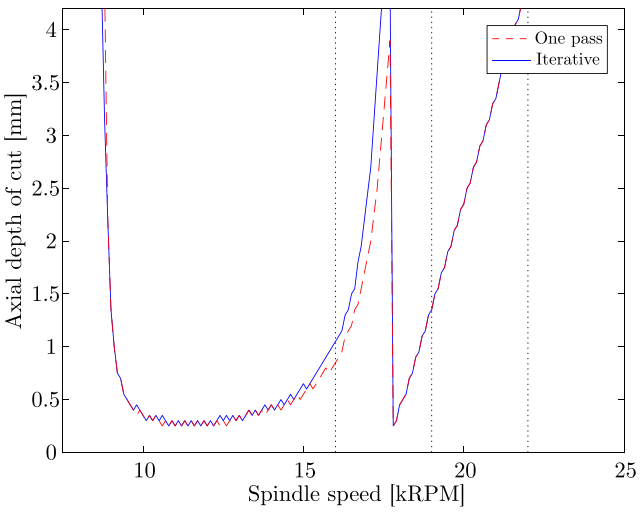

Fig. 26 Comparison of the stability lobes obtained by dynamic simulation using single pass and iterative integration procedures with the default time step

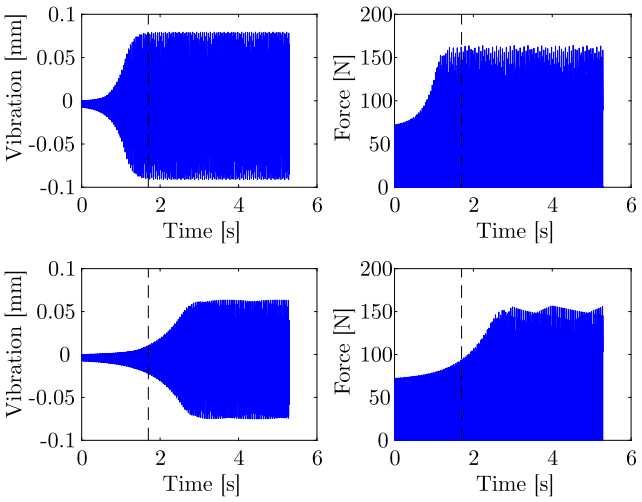

Fig. 27 Evolution of the displacement along feed direction using the default time step at 17,000 rpm spindle speed and 2.4 mm ADOC (top: single pass algorithm, bottom: iterative algorithm)

- As far as the iterative procedure gives more precise results than the one pass algorithm for a given time step and for a given CPU time, it should be the preferred integration procedure.
- The use of the default time step (at least 30 time steps between entry and exit of the workpiece, checking that it provides a sample frequency sufficient to model the high frequency content of the dynamic system) gives reliable results in terms of stability and good precision for the peak to peak amplitude.
- Increasing the time step below the default value can lead to faulty simulations (unstable case considered stable for example), so it should be avoided.

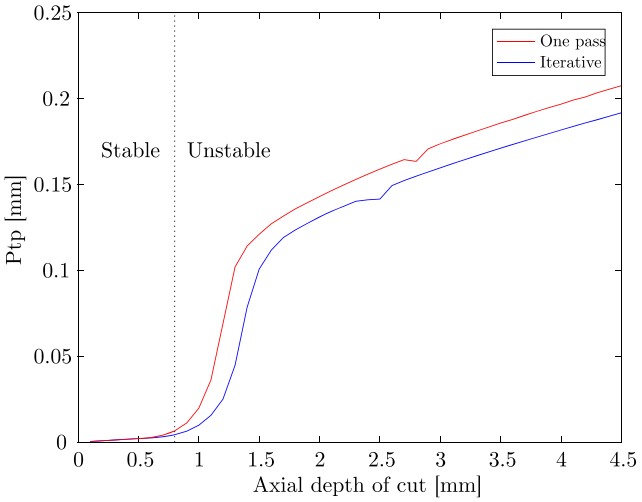

Fig. 28 Evolution of the peak to peak amplitude with respect to the axial depth of cut at a spindle speed of 16,000 rpm (instability linked to Hopf bifurcation)

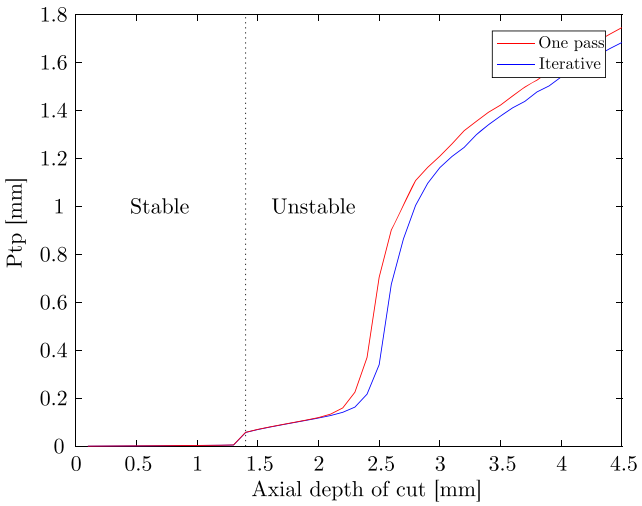

Fig. 29 Evolution of the peak to peak amplitude with respect to the axial depth of cut at a spindle speed of 19,000 rpm (instability linked to flip bifurcation)

- Reducing the time step can lead to higher precision computation but at the cost of higher CPU time (CPU time increases as the square of the number of time steps).

With all those elements, the choice of the default time step with the iterative integration procedure appears as the best compromise as a starting point for the simulation of a milling operation. Using the default time step with the iterative algorithm produces accurate results while some significant discrepancies can be observed with the single pass algorithm. The use of the iterative algorithm with the default time step seems to be a good compromise for accurate simulation with a reasonable simulation time.

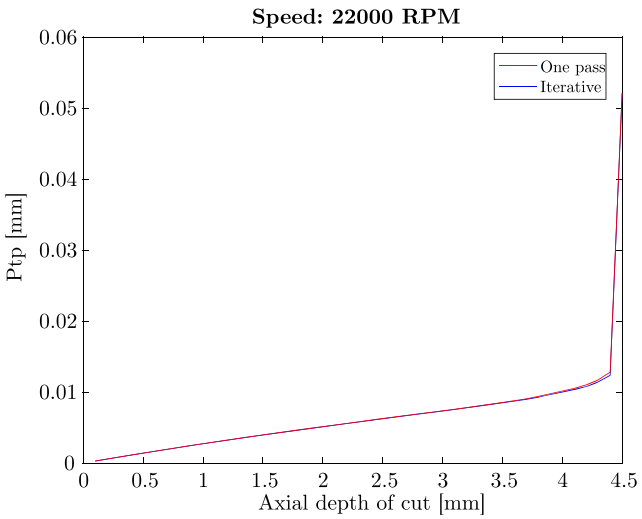

Fig. 30 Evolution of the peak to peak amplitude with respect to the axial depth of cut at a spindle speed of 22,000 rpm

References

1. Tlusty J, Polacek M (1963) The stability of the machine tool against self-excited vibration in machining. ASME Int Res Product 1:465–474
2. Smith S, Tlusty J (1993) Efficient simulation programs for chatter in milling. CIRP Ann Manuf Technol 42:463–466
3. Altintas Y, Budak E (1995) Analytical prediction of stability lobes in milling. CIRP Ann 44:357–362
4. Merdol SD, Altintas Y (2004) Multi frequency solution of chatter stability for low immersion milling. J Manuf Sci Eng 126:459–467
5. Fofana MS (1993) Delay dynamical systems with application to machine-tool chatter. University of Waterloo, department of civile engineering, PhD thesis
6. Johnson MA (1996) Nonlinear differential equations with delay as models for vibrations in the machining of metals. Cornell University, PhD thesis
7. Kalmar-Nagy T, Stepan G, Moon FC (2001) Subcritical hopf bifurcation in the delay equation model for machine tool vibrations. Nonlinear Dyn 26:121–142
8. Insperger T (2002) Stability analysis of periodic delay-differential equations modeling machine tool chatter. Budapest University of Technology and Economics, PhD thesis
9. Ahmadi K, Ismail F (2012) Stability lobes in milling including process damping and utilizing multi-frequency and semi-discretization methods. Int J Mach Tools Manuf 54-55:46–54
10. Lorong P, Micari F, Touratier M (2007) Advances in material forming, chapter modelling of cutting and machining: 10 years of ESAFORM activity. Springer, Paris, pp 225–236
11. Ozel T, Zeren E (2005) Finite element method simulation of machining of aisi 1045 steel with a round edge cutting tool. In: Proceedings of 8th CIRP international workshop on modeling of machining operations, pp 533–541
12. Movahheddy M (2000) Simulation of the orthogonal metal cutting process using an arbitrary Lagrangian-Eulerian finite element method. J Mat Proc Tech 103:267–275
13. Limido J, Espinosa C, Salaün M, Lacome JL (2007) SPH method applied to high speed cutting modelling. Int J Mech Sci 49(7):898–908
14. Arrazola P, Ozel T, Umbrello D, Davies M, Jawahir I (2013) Recent advances in modelling of metal machining processes. CIRP Ann Manuf Technol 62:695–718
15. Cheng K (ed) (2008) Machining dynamics: theory, applications and practices. Springer, London
16. Altintas Y (2012) Manufacturing automation: metal cutting mechanics, machine tool vibrations, and CNC design, 2nd edn. Cambridge University Press
17. Peigne G (2003) A model of milled surface generation for time domain simulation of high-speed cutting. Proc Inst Mech Eng Part B J Eng Manuf 217(7):919–930
18. Campomanes ML, Altintas Y (2003) An improved time domain simulation for dynamic milling at small radial immersion. Trans ASME 125:416–422
19. Engin S, Altintas Y (2001) Mechanics and dynamics of general milling cutters. Part I: Helical end mills. Int J Mach Tools Manuf 41:2195–2212
20. Engin S, Altintas Y (2001) Mechanics and dynamics of general milling cutters. Int J Mach Tools Manuf 41(15):2213–2231
21. Al-Regib E, Ni J, Lee SH (2003) Programming spindle speed variation for machine tool chatter suppression. Int J Mach Tools Manuf 43:1229–1240
22. Seguy S, Insperger T, Arnaud L, Dessein G, Peigne G (2011) Suppression of period doubling chatter in high-speed milling by spindle speed variation. Mach Sci Technol 15:153–171
23. Fei J, Lin B, Yan S, Lan X, Zha X, Zhang, Dai S (2017) Chatter prediction for milling of flexible pocket-structure. Int J Adv Manuf Technol 89:2721–2730
24. Wang M, Gao L, Zheng Y (2014) Prediction of regenerative chatter in the high-speed vertical milling of thin-walled workpiece made of titanium alloy. Int J Adv Manuf Technol 72:707–716
25. Yang Y, Zhang W-H, Ma Y-C, Wan M (2016) Chatter prediction for the peripheral milling of thin-walled workpieces with curved surfaces. Int J Mach Tools Manuf 109:36–48
26. Ko JH (2015) Time domain prediction of milling stability according to cross edge radiuses and flank edge profiles. Int J Mach Tools Manuf 89:74–85
27. Xuewei Z, Tianbiao Y, Wanshan W (2016) Chatter stability of micro end milling by considering process nonlinearities and process damping. Int J Adv Manuf Technol 87:2785–2796
28. Liu Y, Luo Z, Wan Z, Wang, Zhang Y (2017) Chatter stability prediction in milling using time-varying uncertainties. Int J Adv Manuf Technol 89:2627–2636
29. Totis G, Albertelli P, Torta M, Sortino M, Monno M (2017) Upgraded stability analysis of milling operations by means of advanced modeling of tooling system bending. Int J Mach Tools Manuf 113:19–34
30. Wang JJ, Uhlmann E, Oberschmidt D, Sung CF, Perfilov I (2016) Critical depth of cut and asymptotic spindle speed for chatter in micro milling with process damping. CIRP Ann 65:113–116
31. Lee C-H, Yang M-Y, Oh C-W, Gim T-W, Ha J-Y (2015) An integrated prediction model including the cutting process for virtual product development of machine tools. Int J Mach Tools 90:29–43
32. Ming L, Jiawei M, Dinghua Z (2016) Time-domain modeling of a cutter exiting a workpiece in the slot milling process. Chin J Aeronaut 29(6):1852–1858
33. Ko JH (2014) Time domain prediction of side and plunge milling stability considering edge radius effect. Procedia CIRP 14:153–158
34. Li Z, Yang Z, Peng Y, Ming X (2016) Prediction of chatter stability for milling process using runge-kutta-based complete discretization method. Int J Adv Manuf Technol 86:943–952
35. Rubeo MA, Schmitz TL (2016) Global stability predictions for flexible workpiece milling using timedomain simulation. J Manuf Syst 40:8–14
36. Denkena B, Hollman F (2013) Process machine interactions: prediction and manipulation of interactions between manufacturing processes and machine tool structure. Springer Lecture Notes in Production Engineering
37. Altintas Y, Lee P (1996) A general mechanics and dynamics model for helical end mills. CIRP Ann Manuf Technol 45(1):59–64
38. Quintana G, Ciurana J (2011) Chatter in machining processes: a review. Int J Mach Tools Manuf 51:363–376
39. Schmitz TL, Davies MA, Kennedy MD (2001) Tool point frequency response prediction for high speed machining by RCSA. J Manuf Sci Eng 123:700–707
40. Huynh HN, Rivière-Lorphèvre E, Verlinden O (2016) Integration of machining simulation within multibody framework: application to milling. In: Proceedings of the 4th joint international conference on multibody system dynamics
41. Verlinden O, Ben Fekih L, Kouroussis G (2013) Symbolic generation of the kinematics of multibody systems in easydyn: from mupad to xcas/giac. Theor Appl Mech Lett 3(1):013012
42. Delio T, Tlusty J, Smith S (1992) Use of audio signals for chatter detection and control. ASME J Eng Ind 114:146–157
43. Kuljanic E, Sortino M, Totis G (2008) Multisensor approaches for chatter detection in milling. J Sound Vib 312:672–693

44. Shi Y, Mahr F, Wagner U, Uhlmann E (2012) Chatter frequencies of micromilling processes: influencing factors and online detection via piezoactuators. Int J Mach Tools Manuf 56:10–16
45. Ganguli A, Deraemaekar A, Horodinca M, Preumont A (2005) Active damping of chatter in machine tools—demonstration with a hardware in the loop simulator. J Syst Control Eng 219(15):359–369
46. Seguy S, Dessein G, Arnaud L (2008) Surface roughness variation of thin wall milling, related to modal interactions. Int J Mach Tools Manuf 48:261–274
47. Insperger T, Mann BP, Stepan G, Bayly PV (2003) Stability of up-milling and down-milling, part 1: alternative analytical methods. Int J Mach Tools Manuf 43:25–34
48. Insperger T, Mann BP, Stepan G, Bayly PV (2003) Stability of up-milling and down-milling, part 2: experimental verification. Int J Mach Tools Manuf 43:35–43
49. Eynian M (2015) Vibration frequencies in stable and unstable milling. Int J Mach Tools Manuf 90:44–49
50. Insperger T, Stepan G, Bayly PV, Mann BP (2003) Multiple chatter frequencies in milling process. J Sound Vib 262:333–345
51. Insperger T, Stepan G (2000) Stability of high-speed milling. In: Proceedings of symposium on nonlinear dynamics and stochastic mechanics, pp 119–123
52. Graham E, Mehrpouya M, Park SS (2013) Robust prediction of chatter stability in milling based on the analytical chatter stability. J Manuf Process 15:508–517